The Astrophysical Journal, 640:L119–L122, 2006 April 1

THE INFLUENCE OF BARYONS ON THE CLUSTERING OF MATTER AND WEAK-LENSING SURVEYS

Y. P. Jing,[1,2] Pengjie Zhang,[1,2] W. P. Lin,[1,2] L. Gao,[3,4] and V. Springel[3]

Received 2005 December 15; accepted 2006 February 20; published 2006 March 9

ABSTRACT

Future weak-lensing measurements of cosmic shear will reach such high accuracy that second-order effects in weak-lensing modeling, such as the influence of baryons on structure formation, become important. We use a controlled set of high-resolution cosmological simulations to quantify this effect by comparing pure *N*-body dark matter runs with corresponding hydrodynamic simulations, carried out both in nonradiative form and in dissipative form with cooling and star formation. In both hydrodynamic simulations, the clustering of the gas is suppressed while that of dark matter is boosted at scales $k > 1\ h\ \mathrm{Mpc}^{-1}$. Despite this counterbalance between dark matter and gas, the clustering of the total matter is suppressed by up to 1% at $1\ h\ \mathrm{Mpc}^{-1} \lesssim k \lesssim 10\ h\ \mathrm{Mpc}^{-1}$, while for $k \approx 20\ h\ \mathrm{Mpc}^{-1}$ it is boosted, up to 2% in the nonradiative run and 10% in the run with star formation. The stellar mass formed in the latter is highly biased relative to the dark matter in the pure *N*-body simulation. Using our power spectrum measurements to predict the effect of baryons on the weak-lensing signal at scales corresponding to multipole moments $100 < l < 10{,}000$, we find that baryons may change the lensing power spectrum by less than 0.5% at $l < 1000$, but by 1% to 10% at $1000 < l < 10{,}000$. The size of the effect exceeds the predicted accuracy of future lensing power spectrum measurements and will likely be detected. Precise determinations of cosmological parameters with weak lensing, and studies of small-scale fluctuations and clustering, therefore rely on properly including baryonic physics.

Subject headings: cosmology: theory — dark matter — galaxies: formation — gravitational lensing

1. INTRODUCTION

Weak gravitational lensing directly measures the projected mass distribution and is emerging as one of the most powerful and robust probes of the large-scale structure of the universe and the nature of dark matter, dark energy, and gravity (Huterer 2002; Hu 2002; Jain & Taylor 2003; Takada & Jain 2004; Ishak et al. 2005; Knox et al. 2005). Ongoing and upcoming surveys such as CFHTLS,[5] DES,[6] LSST,[7] Pan-STARRS,[8] SKA,[9] and *SNAP*[10] will significantly reduce statistical errors in lensing power spectrum measurements, to the sub-1% level at $l \sim 1000$. As new analysis techniques enable a significant reduction of systematic errors in cosmic shear (Jarvis & Jain 2004; Jain et al. 2005; Heymans et al. 2006; references therein) and cosmic magnification measurements (Ménard & Bartelmann 2002; Scranton et al. 2005; Zhang & Pen 2005, 2006), weak-lensing measurement is entering the precision era. To match this accuracy, many simplifications in theoretical modeling have to be scrutinized in detail (Bernardeau 1998; Schneider et al. 1998; Dodelson & Zhang 2005; Dodelson et al. 2006; White 2005).

A widely adopted simplification in weak-lensing modeling is the assumption that baryons trace dark matter perfectly. With this simplification, weak lensing involves only gravity and collisionless dark matter dynamics, allowing it to be accurately predicted with the aid of *N*-body simulations. However, on small scales baryons do *not* follow the dark matter distribution. Recently, White (2004) and Zhan & Knox (2004) estimated the effects of cooling gas and intracluster gas on the lensing power spectrum, respectively. These two components of baryons can both have an effect of a few percent on the lensing power spectrum at $l \sim 3000$, but with opposite signs. Such effects exceed future measurement errors and are certainly relevant in order to exploit the full power of precision measurements of weak lensing. However, analytical models are simplified with ad hoc parameters and lack the ability to deal with back-reactions of baryons on the dark matter. They cannot robustly answer several key questions, such as (1) to what level the two effects cancel, (2) at what scales each of them dominates, and (3) how large the effect is for the nonvirialized intergalactic medium, where most of the baryons reside. To quantify the effect of baryons on lensing statistics accurately, it is hence necessary to use hydrodynamic simulations with all relevant gas physics included. In this Letter, we analyze a controlled set of simulations to address this issue.

2. BARYONIC EFFECT ON THE CLUSTERING OF COSMIC MATTER

We use the GADGET2 code (Springel et al. 2001; Springel 2005) to simulate structure formation in a concordance cosmological model. The cosmological and initial density fluctuation parameters of the model are $(\Omega_m, \Omega_\Lambda, \Omega_b, \sigma_8, n, h) = (0.268, 0.732, 0.044, 0.85, 1, 0.71)$. Three simulations were run with the same initial fluctuations for a cubic box of $100\ h^{-1}$ Mpc. The first simulation is a pure dark matter cosmological simulation. The second is a gas simulation in which no radiative cooling of gas is considered. The last run is a gas simulation that includes the physical processes of radiative cooling and star formation. It also includes supernova feedback, outflows by galactic winds, and a subresolution multiphase model for the interstellar medium as detailed in Springel & Hernquist (2003). In all simulations, we use 512^3 particles to represent each component of dark matter and gas.

[1] Shanghai Astronomical Observatory, Chinese Academy of Sciences, 80 Nandan Road, 200030 Shanghai, China; ypjing@shao.ac.cn.
[2] Joint Institute for Galaxy and Cosmology of the Shanghai Astronomical Observatory and the University of Science and Technology of China.
[3] Max-Planck-Institut für Astrophysik, Karl-Schwarzschild-Strasse 1, D-85748 Garching, Germany.
[4] Institute for Computational Cosmology, Department of Physics, University of Durham, Science Laboratories, South Road, Durham DH1 3LE, UK.
[5] See http://www.cfht.hawaii.edu/Science/CFHLS.
[6] See http://www.darkenergysurvey.org.
[7] See http://www.lsst.org.
[8] See http://pan-starrs.ifa.hawaii.edu.
[9] See http://www.skatelescope.org.
[10] See http://snap.lbl.gov.

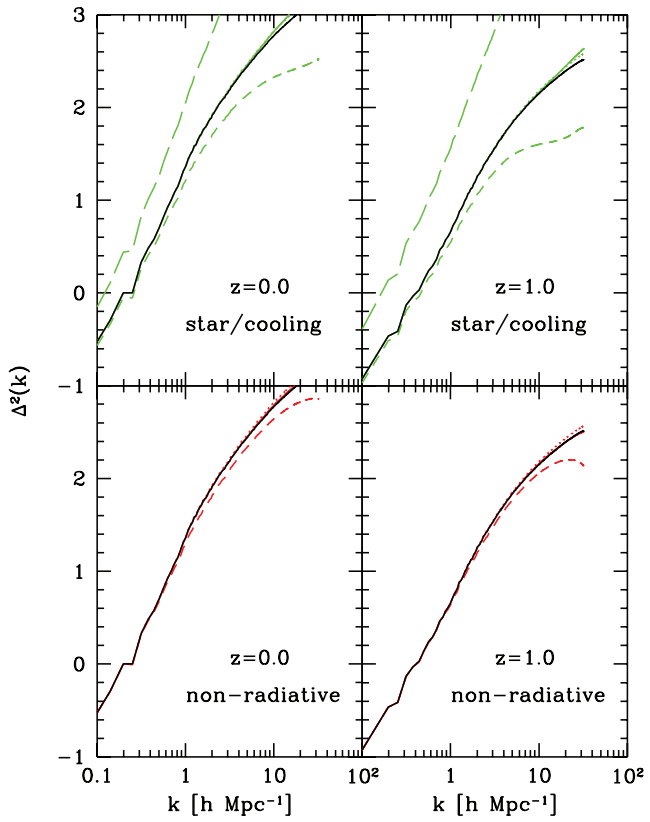

FIG. 1.—Power spectrum of density fluctuations of each matter component in the nonradiative gas simulation (*bottom*) and in the gas cooling and star formation simulation (*top*), at redshifts $z = 1$ and $z = 0$. The results are compared with the spectrum of the pure dark matter simulation (*black solid lines*). The colored dotted lines, short-dashed lines, long-dashed lines, and solid lines are plotted for the dark matter, gas, stars, and total matter density field, respectively.

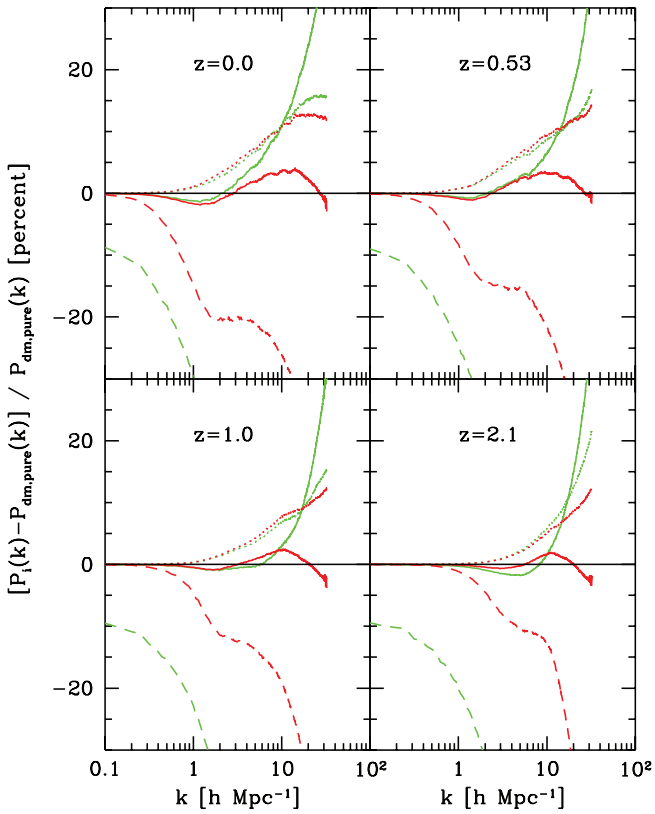

FIG. 2.—Influence of baryons on the clustering of each matter component. The plots show the relative percentage difference of the power spectrum of each matter component in the gas simulations relative to the pure dark matter simulation. The results of the nonradiative run are plotted in red, and those of the star formation run in green. The dotted lines, dashed lines, and solid lines are plotted for the dark matter and gaseous components and the total matter density field, respectively. The stellar component in the star formation run is omitted here, as the difference can be easily inferred from Fig. 1.

Uncertainties in simulating star formation could bias our study. To check the robustness of our star formation run, we measured the stellar mass density Ω_* in units of the critical density at $z = 0$. We found $\Omega_* = 0.0034$. This is in reasonable agreement with recent observational results (e.g., $\Omega_* = 0.0035$, Fukugita et al. 1998; $\Omega_* = 0.0028 \pm 0.0008$, Bell et al. 2003). The star formation history of the simulation is therefore close enough to reality for the purposes of the present Letter.

2.1. *Clustering in the Nonradiative Run*

We measure the mass power spectrum $P(k)$ for matter, gas, and stars separately, as well as for the total matter density in the simulations using the method of Jing (2005). The power spectrum of each matter component is plotted in Figure 1 for redshifts $z = 0$ and $z = 1$. Here we use the mass variance $\Delta^2(k)$ per logarithmic interval in wavelength, which is related to $P(k)$ by $\Delta^2(k) = 4\pi k^3 P(k)/(2\pi)^3$. According to the extensive tests of Hou et al. (2005), the power spectrum is affected by the force resolution at $k > k_\eta \approx 0.3(2\pi/\eta)$, where η is the Plummer-equivalent force softening length used in the simulation. In our simulations, $\eta = 5\ h^{-1}$ kpc for the pure dark matter and nonradiative runs and $\eta = 9\ h^{-1}$ kpc for the star formation run. Down to the scale of $k \approx 20\ h$ Mpc^{-1}, the force resolution should have negligible effects.

Comparing the results of the pure dark matter and the nonradiative runs, one finds that the gas has a weaker clustering than the dark matter on small scales ($k > 1\ h$ Mpc^{-1}). This can be interpreted as the result of gas pressure, which reduces small-scale structure in the gas distribution. Zhan & Knox (2004) approximated the hot baryon distribution by assuming that the gas is in hydrostatic equilibrium in NFW dark halos (Makino et al. 1998) and found a qualitatively similar result. But quantitatively, the gas clustering suppression in their simple analytic estimate is stronger than our simulations indicate. At $k = 10\ h$ Mpc^{-1} and $z = 0$, the $\Delta^2(k)$ of gas is 25% lower than that of dark matter in our nonradiative simulation (see Fig. 2), while the $\Delta^2(k)$ of gas is 50% lower in their analytic estimate. We also see a more extended baryonic effect at $k < 1\ h$ Mpc^{-1}, which may be caused by filaments and is beyond the exploration of their halo model. These effects indicate the need for hydrodynamic simulations to accurately assess the effect of baryons on the clustering of cosmic matter.

An interesting result from our nonradiative simulation is that its dark matter has stronger clustering than found in the pure dark matter run. To show the difference clearly, we plot it separately in Figure 2, where we also show the clustering differences of other matter components relative to the pure dark matter run. The dark matter clustering is a few percent stronger in the nonradiative cooling simulation at $k > 1\ h$ Mpc^{-1} and is more than 10% stronger at $k > 10\ h$ Mpc^{-1}. This behavior can be understood as a result of the gravitational back-reaction due to hot gas, since the gas is hotter than the dark matter virial

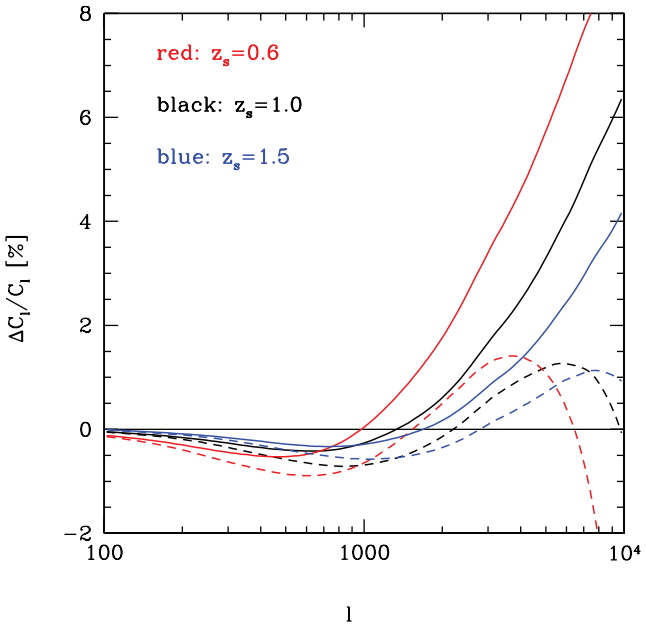

FIG. 3.—Effect of baryons on the shear power spectrum C_l, expressed as a relative percentage difference from the pure dark matter model. Here the source galaxies are assumed to be at redshifts z_s of 0.6, 1.0, and 1.5, respectively. The dashed lines are the predictions from our nonradiative run, while the solid lines give the results for the star formation run.

temperature in the central regions of dark halos, because of its collisional nature (see Rasia et al. 2004; W. P. Lin et al. 2006, in preparation).

Compared with the power spectra of gas and dark matter, the $P_{\rm NR}^{\rm tot}(k)$ of the total matter distribution in the nonradiative run differs less dramatically from the $P_{\rm DM}(k)$ of the pure dark matter run,[11] because the baryonic suppression of the gas clustering is partially counterbalanced by its effect on the dark matter. However, there still exists a significant difference in the total matter clustering between the two runs (see Figs. 1 and 2). The total matter spectrum $P_{\rm NR}^{\rm tot}(k)$ is a few percent lower than $P_{\rm DM}(k)$ at $k \approx 2\ h\ {\rm Mpc}^{-1}$ and is a few percent higher than $P_{\rm DM}(k)$ at $k \approx 10\ h\ {\rm Mpc}^{-1}$. At the smaller scales, the difference becomes smaller because $P_{\rm NR}^{\rm gas}(k)$ drops faster than $P_{\rm NR}^{\rm dm}(k)$ increases. Although the formal gravitational resolution limit of the simulation is $k \approx 40\ h\ {\rm Mpc}^{-1}$, hydrodynamic convergence can only be expected on somewhat larger scales, and thus it will be interesting to check the results at $k > 10\ h\ {\rm Mpc}^{-1}$ shown in Figure 2 with higher resolution simulations.

2.2. *Clustering in the Simulation with Star Formation*

In our star formation run, the stellar matter is found to be significantly more clustered than dark matter or gas (Fig. 1). Its power spectrum $P_{\rm SF}^{\rm star}(k)$ is a few times higher than the dark matter counterpart $P_{\rm SF}^{\rm dm}(k)$, and the bias factor increases toward smaller scales. This result is expected, because the stars can form only in high-density regions and thus are highly biased tracers of the matter distribution.

On the other hand, the power spectrum of gas, $P_{\rm SF}^{\rm gas}(k)$, is significantly lower than $P_{\rm SF}^{\rm dm}(k)$. Apart from the mild effects of shock heating and gas pressure that can be inferred from the nonradiative simulation, the main reason is that gas is underrepresented relative to the dark matter in high-density regions, where part of the gas has cooled and turned into stars. Because of this reverse bias, $P_{\rm SF}^{\rm gas}(k)$ is always smaller by ~10% than $P_{\rm SF}^{\rm dm}(k)$, even on large scales (Fig. 2), and drops much faster at small scales than the counterpart $P_{\rm NR}^{\rm gas}(k)$ in the nonradiative run. The power spectrum of dark matter $P_{\rm SF}^{\rm dm}(k)$ looks very similar to the counterpart $P_{\rm NR}^{\rm dm}(k)$ in the nonradiative run, except that the former is higher at $k > 10\ h\ {\rm Mpc}^{-1}$ because of the baryon condensation in the star formation run.

The power spectrum of the total matter density $P_{\rm SF}^{\rm tot}(k)$ shows a similar decrease at $k \lesssim 2\ h\ {\rm Mpc}^{-1}$ to that found in the nonradiative run. As we discussed above, this behavior is mainly due to shock heating and the thermal pressure of the gas. This is confirmed in our star formation run, indicating that this feature is robust against the star formation processes. The $P_{\rm SF}^{\rm tot}(k)$ is higher than $P_{\rm NR}^{\rm tot}(k)$ at $k > 10\ h\ {\rm Mpc}^{-1}$ at $z < 1$, which is mainly caused by the baryon condensation due to gas cooling. We also note that $P_{\rm SF}^{\rm tot}(k)$ is slightly lower at $k \approx 8\ h\ {\rm Mpc}^{-1}$ than the counterparts $P_{\rm NR}^{\rm tot}(k)$ and $P_{\rm DM}(k)$ at $z \gtrsim 1$, which likely results from the feedback heating due to active star formation at high redshift.

3. THE BARYONIC EFFECT ON WEAK LENSING

In this section, we study the influence of baryons on the weak-lensing shear power spectrum C_l. We use Limber's approximation (Limber 1954) to calculate C_l from the simulated $P^{\rm tot}$. For a flat universe, C_l and $P^{\rm tot}$ are related by

$$C_l = \left(\frac{3\Omega_m H_0^2}{2c^2}\right)^2 \int P^{\rm tot}\left(\frac{l}{\chi}, z\right) W^2(\chi, \chi_s)\chi^{-2}\, d\chi, \qquad (1)$$

where $W(\chi, \chi_s) = (1+z)\chi(1-\chi/\chi_s)$ is the lensing kernel and χ_s and χ are the comoving angular diameter distances to the source and lens, respectively.

In Figure 3, we show the effect of the baryons on the weak-lensing power spectrum by assuming that the lensed sources are at redshifts z_s of 0.6, 1.0, and 1.5, respectively. For the nonradiative run, the lensing power signal is suppressed by less than 1% at $100 < l < 1000$ and is then enhanced to about 1% at $l = 4000$. The detailed behavior depends on the source redshift, and the relative change of C_l increases with the decrease of z_s. This is expected, since the baryons have more significant effects at lower redshifts (Fig. 2).

Including more realistic star formation processes compensates for the lensing power suppression at $100 < l < 1000$ seen in the nonradiative run. As a result, the change in the lensing power due to the presence of baryons is smaller than 0.5% for $z_s > 0.6$ and $100 < l < 1000$. But at $1000 < l < 10{,}000$, the baryons can increase C_l by up to 10%, depending on z_s. Again, the relative change of C_l increases with the decrease of z_s.

Compared with the previous study by Zhan & Knox (2004) for the effect of hot baryons, our prediction for $\Delta C_l/C_l$ in the nonradiative run is quite different from their finding of a monotonic decline of $\Delta C_l/C_l$ with l at $l > 1000$. We argue that the main reason for this is that they neglected the back-reaction of the thermal baryons on the dark matter in their analytical modeling.

To match the accuracy of future lensing surveys, the matter power spectrum at the scales discussed in this Letter must be calibrated to ~1% accuracy (Huterer & Takada 2005). Thus, the baryonic effect is nonnegligible for future lensing analysis. Here we perform a simple estimate to demonstrate this point.

[11] Here we use the subscripts DM, NR, and SF for the pure dark matter, nonradiative, and star formation runs, respectively, and the superscripts "dm," "gas," "star," and "tot" for each matter component.

The statistical errors of lensing power spectrum measurements (assuming Gaussianity) are

$$\frac{\Delta C_l}{C_l} = 1\% \left(\frac{l}{1000}\frac{\Delta l}{100}\frac{f_{\rm sky}}{0.1}\right)^{-1/2} \left(1 + \frac{\gamma_{\rm rms}^2}{\bar{n}_g C_l}\right), \qquad (2)$$

where n_g is the galaxy number density, with typical value $\lesssim$100 arcmin^{-2}, and $\gamma_{\rm rms} \sim 0.2$ is the rms fluctuation caused by galaxy ellipticities. At $l \lesssim 3000$, the shot-noise term is subdominant. For future lensing missions with fractional sky coverage $f_{\rm sky} \gtrsim 0.1$, changes in C_l caused by baryons will be comparable to or larger than statistical errors at $l \gtrsim 1000$. To constrain cosmology using measured C_l's at all accessible scales (l less than several times 10^4), the effects due to baryons have to be taken into account; otherwise, the derived constraints can be biased. For example, since $C_l \propto \Omega_m^{\sim 1.2}\sigma_8^2$ (e.g., Van Waerbeke et al. 2001), neglecting this effect can lead to an overestimate of $\Omega_m^{\sim 0.6}\sigma_8$ by several percent. It can also cause an overestimate of the initial power index n. To avoid such biases, accurate modeling of the baryonic effects using hydrodynamic simulations is required. On the other hand, a precision measurement of the lensing signal at an l of about a few thousand could be used to observationally determine the baryonic effects and to constrain the galaxy formation process.

4. CONCLUSIONS

In this Letter, we used a controlled set of high-resolution N-body and hydrodynamic/N-body simulations to study the influence of baryons on the clustering of cosmic matter. Since the three simulations we used have identical initial conditions, the simulated power spectra suffer essentially the same sample variance. Since we quantify the baryonic effect as ratios of corresponding power spectra, the result presented in this Letter is effectively free of sample variance. In both the nonradiative simulation and the simulation with gas cooling and star formation, the clustering of the gas is suppressed while that of dark matter is boosted at $k > 1\ h$ Mpc^{-1}. The stellar mass is highly biased relative to the dark matter in the pure N-body simulation. Despite a partial counterbalance between the dark matter and the gas, the clustering of the total matter is suppressed by up to 1% at $1\ h\ {\rm Mpc}^{-1} \lesssim k \lesssim 10\ h\ {\rm Mpc}^{-1}$ and is boosted by up to 2% in the nonradiative run, and 10% in the star formation run at $k \approx 20\ h$ Mpc^{-1}. Using these power spectrum measurements to study the baryonic effect on weak-lensing shear measurements at $100 < l < 10{,}000$, we find that baryons can change the shear power spectrum by less than 0.5% at $l < 1000$ but by 1% to 10% at $1000 < l < 10{,}000$. Therefore, the influence of baryons on the clustering of cosmic matter will be detected in future weak-lensing surveys. Understanding these baryonic effects is not only important for galaxy formation, but also crucial for accurately determining cosmological parameters with cosmic shear, and for constraining the initial fluctuations on small scales.

The simulations were run at Shanghai Supercomputer Center. The work at Shanghai is supported by grants from the National Natural Science Foundation of China (Nos. 10125314, 10373012, 10533030) and from Shanghai Key Projects in Basic Research (No. 04JC14079 and 05XD14019). P. Z. is supported by the One Hundred Talents project of the Chinese Academy of Sciences.

REFERENCES

Bell, E. F., McIntosh, D. H., Katz, N., & Weinberg, M. D. 2003, ApJS, 149, 289
Bernardeau, F. 1998, A&A, 338, 375
Dodelson, S., Shapiro, C., & White, M. 2006, Phys. Rev. D, 73, 023009
Dodelson, S., & Zhang, P. 2005, Phys. Rev. D, 72, 083001
Fukugita, M., Hogan, C. J., & Peebles, P. J. E. 1998, ApJ, 503, 518
Heymans, C., et al. 2006, MNRAS, in press (astro-ph/0506112)
Hou, Y. H., Jing, Y. P., Zhao, D. H., & Börner, G. 2005, ApJ, 619, 667
Hu, W. 2002, Phys. Rev. D, 66, 083515
Huterer, D. 2002, Phys. Rev. D, 65, 063001
Huterer, D., & Takada, M. 2005, Astropart. Phys., 23, 369
Ishak, M., Upadhye, A., & Spergel, D. N. 2005, preprint (astro-ph/0507184)
Jain, B., Jarvis, M., & Bernstein, G. 2005, J. Cosmology Astropart. Phys, [2006](2), No. 1
Jain, B., & Taylor, A. 2003, Phys. Rev. Lett., 91, 141302
Jarvis, M., & Jain, B. 2004, ApJ, submitted (astro-ph/0412234)
Jing, Y. P. 2005, ApJ, 620, 559
Knox, L., Song, Y.-S., & Tyson, J. A. 2005, Phys. Rev. Lett., submitted (astro-ph/0503644)
Limber, D. N. 1954, ApJ, 119, 655
Makino, N., Sasaki, S., & Suto, Y. 1998, ApJ, 497, 555
Ménard, B., & Bartelmann, M. 2002, A&A, 386, 784
Rasia, E., Tormen, G., & Moscardini, L. 2004, MNRAS, 351, 237
Schneider, P., Van Waerbeke, L., Jain, B., & Kruse, G. 1998, MNRAS, 296, 873
Scranton, R., et al. 2005, ApJ, 633, 589
Springel, V. 2005, MNRAS, 364, 1105
Springel, V., & Hernquist, L. 2003, MNRAS, 339, 289
Springel, V., Yoshida, N., & White, S. D. M. 2001, NewA, 6, 79
Takada, M., & Jain, B. 2004, MNRAS, 348, 897
Van Waerbeke, L., et al. 2001, A&A, 374, 757
White, M. 2004, Astropart. Phys., 22, 211
———. 2005, Astropart. Phys., 23, 349
Zhan, H., & Knox, L. 2004, ApJ, 616, L75
Zhang, P., & Pen, U.-L. 2005, Phys. Rev. Lett., 95, 241302
———. 2006, MNRAS, 367, 169